sustainability

MDPI

Article

Sources Analysis and Health Risk Assessment of Heavy Metals in Street Dust from Urban Core of Zhengzhou, China

Minghao Ren [1,2], Yali Deng [1], Wenshan Ni [3], Jingjing Su [1], Yao Tong [1], Xiao Han [1], Fange Li [1], Hongjian Wang [1,2], Fei Zhao [1,2], Xiaoxiao Huang [1,2,*] and Zhiquan Huang [4,*]

1 College of Geosciences and Engineering, North China University of Water Resource and Electric Power, Zhengzhou 450046, China; renmh@ncwu.edu.cn (M.R.); dengyali0929@163.com (Y.D.); x20231020204@stu.ncwu.edu.cn (J.S.); z20231020273@stu.ncwu.edu.cn (Y.T.); 16696170962@163.com (X.H.); lifg0602@163.com (F.L.); wanghj@ncwu.edu.cn (H.W.); zhaofei_183@126.com (F.Z.)
2 Henan Joint International Laboratory of Collapse-Landslide-Debris Flow Monitoring and Early Warning, North China University of Water Resources and Electric Power, Zhengzhou 450046, China
3 Zhengzhou Institute of Multipurpose Utilization of Mineral Resources, China Geological Survey, Zhengzhou 450006, China; ni44622725@sohu.com
4 Luoyang Institute of Science and Technology, Luoyang 471023, China
* Correspondence: huangxiaoxiao@ncwu.edu.cn (X.H.); huangzhiquan@ncwu.edu.cn (Z.H.)

Abstract: Fifty-one street dust samples were systematically collected from the urban core of Zhengzhou, China, and analyzed for potentially toxic metals. The concentrations of vanadium (V), manganese (Mn), copper (Cu), zinc (Zn), arsenic (As), lead (Pb), and nickel (Ni) in the samples surpassed the background values of the local soil, indicating a notable potential for contamination. Spatially, the traffic area was the most polluted with a total heavy metal concentration of Cu, Zn, As, Pb, and Ni, while the pollution levels were lower in the culture and education area and commercial area with total concentrations of V and Mn. Seasonal variations were discerned in the concentrations of heavy metals, with V, Cu, Zn, and As exhibiting heightened levels during the fall and winter, while Mn, Ni, and Pb reached peaks in the spring season. Zn exhibited the highest mean geo-accumulation index (I_{geo}) value at 2.247, followed by Cu at 2.019, Pb at 0.961, As at 0.590, Ni at 0.126, Mn at −0.178, and V at −0.359. The potential ecological risk index (RI) in the traffic-intensive area markedly exceeded other functional areas. Health risk assessments showed that children were more vulnerable to heavy metal exposure than adults, particularly through the ingestion pathway. Correlation analysis, principal component analysis (PCA), and cluster analysis (CA) were applied in conjunction with the spatial–temporal concentration patterns across various functional areas to ascertain the plausible sources of heavy metal pollutants. The results indicated that heavy metals in the urban street dust of Zhengzhou were multifaceted, stemming from natural processes and diverse anthropogenic activities such as coal burning, industrial emissions, traffic, and construction operations.

Keywords: heavy metal pollution; urban street dust; seasonal variations; source identification; health risk assessment

check for updates

Citation: Ren, M.; Deng, Y.; Ni, W.; Su, J.; Tong, Y.; Han, X.; Li, F.; Wang, H.; Zhao, F.; Huang, X.; et al. Sources Analysis and Health Risk Assessment of Heavy Metals in Street Dust from Urban Core of Zhengzhou, China. *Sustainability* **2024**, *16*, 7604. https://doi.org/10.3390/su16177604

Academic Editor: Konstantinos Dimitriou

Received: 17 July 2024
Revised: 21 August 2024
Accepted: 29 August 2024
Published: 2 September 2024

Copyright: © 2024 by the authors. Licensee MDPI, Basel, Switzerland. This article is an open access article distributed under the terms and conditions of the Creative Commons Attribution (CC BY) license (https://creativecommons.org/licenses/by/4.0/).

1. Introduction

Constituting a significant component of particle environmental contaminants, street dust is defined as the sediment that accumulates on the street surface [1,2]. As urbanization and industrialization progress rapidly, street dust has steadily attracted considerable attention in the study of urban surface pollution. Investigations have indicated that the dispersion and aggregation of street dust stem from diverse sources, encompassing both natural sources like wind dispersal, atmospheric deposition, and precipitation runoff, as well as anthropogenic activities including vehicular traffic (emissions, mechanical abrasion from vehicle components, and road degradation), urban development (erosion and deterioration of painted surfaces and demolition operations), agricultural practices (application of

pesticides and herbicides), and industrial processes (combustion of fossil fuel and metal refining) [3–7].

A multitude of hazardous pollutants, particularly heavy metals, are prevalent within street dust particulates [8,9]. These particulates have the potential to be assimilated by humans through inhalation, ingestion, and dermal contact pathways [10]. Heavy metals exhibit toxicity, persistence, and resistance to degradation [11,12], thus posing enduring health risks upon prolonged accumulation within the body. Lead (Pb), for instance, is renowned for its deleterious effects on human health upon excessive exposure, manifesting in direct damage to brain cells, resulting in fetal mental impairment, cognitive decline, and potentially fatal consequences for the elderly [13]. Furthermore, protracted exposure to As and Ni carries carcinogenic, teratogenic, and mutagenic implications [14]. Excessive intake of Cu may induce irreversible harm to human physiology [15,16]. Children were found to be more vulnerable to potential carcinogenic health risks arising from heavy metals [17–19]. Additionally, highly toxic heavy metals such as lead, chromium, arsenic, and cadmium can be adsorbed onto the surface of dust particles, rendering them resistant to decomposition in water [20]. Street dust on impermeable paved surfaces is subsequently transported by rainwater, infiltrating the water circulation system [21]. This process could contaminate both water bodies and soils, posing a significant threat to ecological integrity [22,23]. Therefore, it is necessary to investigate the characteristics of heavy metals in urban dust and assess the potential risks to human health.

Since the 1970s, numerous studies have been conducted to investigate the concentrations and spatial distributions of heavy metals, identify sources, and assess health risks in urban environments [18,24–27]. The concentrations of heavy metals in street dust were mainly controlled by anthropogenic activities [28,29]. Therefore, the heavy metal concentrations vary significantly across functional areas. Heavy traffic areas, commercial zones, and industrial parts of the urban core are usually enriched in heavy metals [4,30,31]. Locations close to heavily congested roads are severely polluted by Pb, Zn, Cu, and Cd from traffic [32,33], while industrial activities contribute Cu, Zn, Mn, Cd, Pb, Ni, and Cr to the street dust [10,28]. The concentrations of heavy metals were also observed to vary between different seasons, mainly controlled by the local climate [34–36]. Generally, minor accumulations of pollutants were observed in summer, mainly associated with the high temperature, rainfall, and relatively strong diffusion capacity. However, the street dusts were enriched in heavy metals during winter, which was due to the poor mobility of dry air and increase in fuel burning for heating [37,38]. Heavy metals such as Cu, Zn, Ni, Pb, and Cr are well studied in previous investigations, while less data on As and V has been reported. As and V are carcinogenic, posing potential risks to human health. As, in particular, has been related to various types of cancer [10,14]. V was recognized as an indicator of oil combustion, crucial for assessing environmental pollution [39,40]. Thus, conducting a comprehensive study on heavy metal concentrations in urban street dust plays an important role in assessing urban environmental quality and human health.

Zhengzhou served as a crucial transportation hub and central city in north China. However, few investigations were conducted on the level of pollution of heavy metals in Zhengzhou's street dust [41]. Additionally, previous studies generally focused on pollutant accumulation at a certain time, but long-term monitoring was absent for the research of seasonal variations, which was necessary for the comprehensive evaluation of heavy metal pollution [28]. In this study, street dust samples were systematically collected from three distinct functional zones in Zhengzhou during March, June, September, and December of 2019. The concentrations of heavy metals in these samples were determined to (1) investigate the spatial and temporal distribution of heavy metals (V, Mn, Cu, Zn, As, Pb, and Ni) across different functional zones; (2) assess the contamination levels of heavy metals in the urban environment; (3) evaluate the human health risks associated with heavy metal exposure, both non-carcinogenic and carcinogenic; and (4) identify potential sources of heavy metals in the street dust of Zhengzhou.

2. Materials and Methods

2.1. Study Area and Sample Collection

Zhengzhou, the capital of Henan Province (Figure 1a), is located in the north-central region of China, which comprises twelve administrative districts (counties and county-level cities), with five districts forming the urban core (Figure 1b). Bounded by Songshan Mountain to the south and west, with lower terrain to the east, Zhengzhou's central urban area covered 1181.51 km^2 by 2019, with a built-up area of 651.35 km^2 and an urban population of 10,352,000 [42]. As one of the national central cities in China, Zhengzhou boasts a well-developed road network and efficient transportation infrastructure [43]. The quantity of motorized vehicles has increased to over 4.5 million, while that of non-motorized vehicles has exceeded 3 million [41]. Because of the typical temperate monsoon climate, the city experiences distinct seasonal variations, characterized by a dry and sandy spring, a hot and humid summer, a crisp fall, and a chilly and rainy winter.

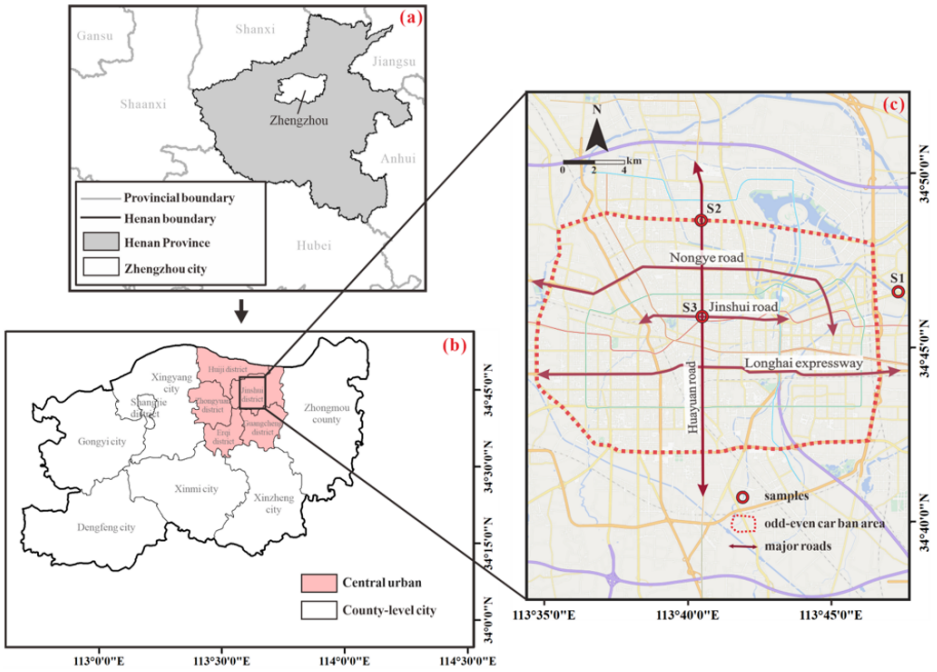


Figure 1. Sampling sites in the study area. (**a**) Location of Zhengzhou city in Henan. (**b**) Central urban region of Zhengzhou city and its county-level cities. (**c**) Study area and sampling sites in Zhengzhou, China. Note: S1, culture and education area; S2, traffic area; S3, commercial area.

In this study, three typical functional zones across Zhengzhou's central urban area (Figure 1c) were investigated: (1) the culture and education area (S1), situated at the intersection of Wenyuan South Road and Jinshui East Road, beyond the 3rd ring road in central Zhengzhou, characterized by relatively lower traffic volume; (2) the traffic area (S2), located at the intersection of Huayuan North Road and the northern 3rd ring road (sampling sites under the Huayuan Road overpass and near the tunnels), falling on the boundary of the traffic restriction zone and experiencing heavy traffic flow; and (3) the commercial area (S3), located near the Zijingshan shopping district, marked by intense pedestrian and vehicular activities, at the intersection of Huayuan Road and Jinshui Road (sampling sites under the Zijingshan overpass).

The urban street dust samples were collected on the three sites in March (4th, 11th, 18th, and 25th), June (3rd and 17th), July (1st), September (2nd, 9th, 16th, 23rd, and 30th), and December (3rd, 10th, 16th, 23rd, 30th) of 2019, covering all four seasons in Zhengzhou. The street dust samples were collected with a brush and a plastic shovel. Three to five dust subsamples at each site were collected within 2–10 m^2 of the roadsides to ensure the sample's representativeness. These subsamples were combined and stored in a

polyethene bag. [44]. Subsequently, these samples were air-dried in a ventilated area for one to two weeks. Following sieving through a 1 mm nylon sieve to eliminate extraneous materials such as hair, roots, cigarette butts, and stones, the dust samples were crushed in an agate mortar and further sieved through a 200-mesh (75 μm) nylon sieve. These prepared samples were then sealed and earmarked for further analysis [45].

2.2. Geochemical Analysis

The handheld X-ray fluorescence (XRF) analyzer, widely applied in geochemical investigations, recycling industries, and food analysis, offers rapid and precise element analysis capabilities [46]. In this study, a handheld XRF analyzer (Olympus VANTA VLW model) in the North China University of Water Resource and Electric Power (Zhengzhou, China) was employed to detect concentrations of heavy metals (V, Mn, Cu, Zn, As, Pb, and Ni) in street dust following the procedure reported by [47]. Before XRF analysis, standard samples were used for calibration. The quality control measures were implemented throughout the analysis process. To ensure result accuracy, the analytical procedure was repeated five times with each sample, and the average value of concentration was calculated. Consistency in instrument settings and conditions was maintained to mitigate errors arising from disparate testing environments and other variables. Replicate XRF measurements typically give RSDs of 5% or less.

2.3. Pollution Level Assessment

The geo-accumulation index (I_{geo}), originally proposed by Müller in 1969 [48], has been widely used for calculating the degree of metal contamination in sediments and soils [49]. I_{geo} accounts for both natural and anthropogenic contributions [50]. The I_{geo} index is given as

$$I_{\text{geo}} = \log_2\left(\frac{\text{C}_n}{\text{kB}_n}\right) \quad (1)$$

where C_n denotes the concentration of metal n, and B_n denotes the background concentration of the study area for metal n. The constant 1.5 (denoted as factor k) is utilized to mitigate the influence of background variations resulting from natural fluctuations or minor anthropogenic inputs [51]. In this study, the background values of the heavy metals in Zhengzhou were reported by [52] for assessment of the geo-accumulation index. According to Muller (1969) [48], the geo-accumulation index has seven classes. Details are shown in Table S1.

The potential ecological risk index (RI), proposed by Hakanson in 1980 [53], is defined as the summation of the individual potential ecological risk factors (Er^i). RI serves to assess the environmental impact stemming from metals present in road dust. Er^i and RI were computed by the following equations [54]:

$$\text{C}_f^i = \frac{\text{C}_{0-1}^i}{\text{C}_n^i} \quad (2)$$

$$\text{Er}^i = \text{Tr}^i \times \text{C}_f^i \quad (3)$$

$$\text{RI} = \Sigma\text{Er}^i \quad (4)$$

where C_{0-1}^i denotes the measured concentration of metal i ($\text{mg}\cdot\text{kg}^{-1}$) and C_n^i denotes the soil background value of metal i ($\text{mg}\cdot\text{kg}^{-1}$). Tr^i is the toxicity coefficient assigned to each metal (V = 2, Mn = 1, Cu = 5, Zn = 1, As = 10, Pb = 5, Ni = 5) [53–56]. The values of Er^i, RI, and their categories are presented in Table S2 [21,53,57].

2.4. Health Risk Assessment

The health risk assessment model, proposed by the U.S. Environmental Protection Agency (USEPA) [58–60], is widely applied for evaluating exposure to pollutants present

in street dust (e.g., heavy metals) through three exposure pathways (ingestion, inhalation, and dermal absorption), which may lead to both carcinogenic and non-carcinogenic health risks [61]. The health risk assessment process encompasses several key steps, including data estimation, the evaluation of exposure pathways, a toxicity assessment, and an overall health risk evaluation [7]. V, Mn, Cu, Zn, As, Pb, and Ni are associated with chronic non-carcinogenic risks, while As and Ni additionally pose carcinogenic risks [62–64].

According to the health risk assessment model, the public may be exposed to heavy metal pollution via three pathways: hand-to-mouth ingestion, inhalation, and dermal contact [25,65]. For non-carcinogenic risks, the average daily dosage can be calculated by the following equations under each exposure pathway for both children and adults [62]:

$$ADD_{ing} = C \times \frac{IngR \times EF \times ED}{BW \times AT} \times 10^{-6} \quad (5)$$

$$ADD_{inh} = C \times \frac{InhR \times EF \times ED}{PEF \times BW \times AT} \quad (6)$$

$$ADD_{dermal} = C \times \frac{SA \times SL \times ABS \times EF \times ED}{BW \times AT} \times 10^{-6} \quad (7)$$

where ADD_{ing}, ADD_{inh}, and ADD_{dermal} ($mg \cdot kg^{-1} \cdot d^{-1}$) denote the average daily dosages through hand–oral ingestion, inhalation, and dermal contact, respectively. C ($mg \cdot kg^{-1}$) denotes the concentration of heavy metal in road dust, and IngR and InhR refer to hand–oral ingestion rate and inhalation rate ($mg \cdot d^{-1}$), respectively. EF represents exposure frequency ($d \cdot a^{-1}$), ED denotes exposure duration, SA signifies exposed skin area, SL represents skin adherence factor, ABS is the dermal absorption factor, PEF is the particle emission factor, BW is the average body weight, and AT denotes average exposure time. These parameters are listed in Table S3.

The hazard quotient (HQ), used to measure the non-cancer risk for both children and adults, is a ratio of the average daily exposure dosage (ADD) to the specific reference dose (RfD) for an individual metal (Equation (8). Generally, the RfD serves as an estimate of daily exposure to a particular substance that is unlikely to result in significant adverse effects over a lifetime [66]. The Hazard Index (HI), which comprises the summary of HQ values, is employed to evaluate the cumulative non-carcinogenic risk across multiple exposure pathways for a given pollutant (Equation (9) [67]. The values of RfD are listed in Table S4 [62,68–71].

$$HQ_i = \frac{ADD_{ing/inh/dermal}}{RfD} \quad (8)$$

$$HI = \sum_{i=1}^{n} HQ_i \quad (9)$$

If the HI value < 1, the risk is considered low or negligible. If HI > 1, there may be a cause for concern regarding potential non-carcinogenic risk [60,72].

For carcinogenic risk, the lifetime average daily dose (LADD) for the Ni and As inhalation exposure route was used to estimate the cancer risk, calculated with the following Equation (10) [4,73]:

$$LADD = C \times \frac{EF}{PEF \times AT} \times \left(\frac{InhR_{child} \times ED_{child}}{BW_{child}} + \frac{InhR_{adult} \times ED_{adult}}{BW_{adult}} \right) \quad (10)$$

where $InhR_{child}$ and $InhR_{adult}$ refer to the inhalation rate for children and adults, respectively. ED_{child} and ED_{adult} refer to exposure duration for children and adults, respectively. BW_{child} and BW_{adult} are the average body weights for children and adults, respectively.

Furthermore, carcinogenic risk (CR) is employed to evaluate the potential health risks posed by metals [74,75]. The calculation of CR is given in Equation (11) [76]:

$$CR = LADD \times SF \quad (11)$$

where SF ($mg \cdot kg^{-1} \cdot d^{-1}$) is the slope factor for carcinogenic exposure [62]. In this study, CR was evaluated only for As and Ni. CR values below 10^{-6} indicate a mild carcinogenic risk, which is negligible. Values ranging from 10^{-6} to 10^{-4} suggest the metal poses an acceptable carcinogenic risk. Conversely, values exceeding this range indicate potential lifetime cancer risks, which are deemed unacceptably high [77]. The values of SF are listed in Table S4 [62,68–71].

3. Results and Discussion

3.1. Characteristics of Heavy Metals in Street Dust of Zhengzhou

Soil background values denote the concentrations of elements in soil unaffected by human activity [78]. The XRF analytical results for heavy metals in the street dust of Zhengzhou are listed in Table 1. In general, the concentrations of the seven heavy metals exceeded their respective soil background values in Zhengzhou, suggesting potential influences from anthropogenic activities. In particular, the mean levels of Zn and Cu exceeded their corresponding background values by 7.33 and 6.5 times, respectively. As and Pb were 2.9 and 2.99 times higher than their background levels, respectively. V, Mn, and Ni concentrations were slightly elevated above their soil background values.

Table 1. Heavy metal concentrations in the urban dusts of Zhengzhou (mg/kg, dry weight).

Study Areas		V	Mn	Cu	Zn	As	Pb	Ni
Culture and education area (S1)	Mean	80.4	518	80.1	245	13.2	53.4	36.2
	SD	13.0	110	30.1	50.6	3.53	16.5	6.74
	Maximum	111	736	133	362	20.0	86.0	47.0
	Minimum	61.0	321	38.0	155	9.00	33.0	27.0
Traffic area (S2)	Mean	77.2	589	121	503	33.7	56.6	37.6
	SD	13.2	164	100	267	31.3	8.15	11.5
	Maximum	98.0	1118	354	1254	118	73.0	67.0
	Minimum	51.0	333	34.0	276	10.0	45.0	26.0
Commercial area (S3)	Mean	70.5	589	110	303	23.6	51.5	31.9
	SD	14.0	76.6	85.3	228	16.4	9.72	6.89
	Maximum	95.0	704	364	916	58.0	63.0	45.0
	Minimum	49.0	481	40.0	146	10.0	34.0	25.0
Overall sites	Median	79.0	549	75.0	271	15.0	53.0	35.0
	SD	13.8	124	79.5	230	21.4	12.0	8.66
	Mean	76.1	565	105	350	23.2	53.9	35.3
Zhengzhou Background *		64.0	417	14.0	42.0	8.00	18.0	21.0

* Background values in soil of Zhengzhou, China [52]. Note: SD, standard deviation. Overall sites (N = 51), include culture and education area (S1) (N = 17), traffic area (S2) (N = 17), and commercial area (S3) (N = 17).

Figure S1 presents the mean concentrations of heavy metals in street dust from some cities in China and other countries. Concentrations in urban street dust are closely linked to the degree of industrial and urban development processes in the city [16,62,79,80]. Famous metropolitan areas like London, Shanghai, and Guangzhou exhibit higher metal concentrations in their street dust [20,81,82]. For the high-level industrialization city, Rafsanjan in Iran, the enrichment of Cu and As in street dust is due to mining [57]. As one of the most important production bases for batteries and relevant raw materials in China, Xinxiang has a high content of As [83]. The concentrations for Mn and As in this study are close to those of megacities such as Shanghai and Guangzhou, while Pb, Ni, Cu, and Zn exhibit lower content levels, resembling those in Beijing [84]. According to Wei et al. (2015) [69], the levels of heavy metals in road dust in Beijing, one of the most densely populated cities in the world, were lower than values from Shanghai and Guangzhou. It may be attributed to the diversion of non-capital functions in Beijing. The lower polluted level of heavy metal in the street dust of Zhengzhou indicates less developed urbanization and industrialization compared with megacities and industrial cities. Notably,

Faisal et al. (2021) [43] investigated the levels of eight heavy metals in the PM2.5 portion of road dust samples collected from various land-use areas in Zhengzhou. The average levels of Cu, Ni, Zn, As, and Pb were found to be 25.13 mg/kg, 12.51 mg/kg, 152.35 mg/kg, 11.53 mg/kg, and 52.15 mg/kg, respectively, all of which were lower than those reported in this study. This indicates that the heavy metal is not only absorbed in the PM2.5 portion of road dust. PM10 particles in road dust were also reported to absorb heavy metals significantly (such as Ni, Zn, As, Co, etc.) [85–87].

3.2. Heavy Metal Concentrations in Different Functional Areas

Spatially, total concentrations of heavy metals varied across the three studied functional areas. The traffic area (S2) was the most polluted in terms of the total concentration of heavy metals of Cu, Zn, As, Pb, and Ni, while the pollution levels were lower in the culture and education area (S1) and commercial area (S3), regarding the total concentrations of V and Mn, respectively (Figure 2). For Cu, Zn, and As, the highest mean content was observed in the traffic zone, with values of 121 mg/kg, 503 mg/kg, and 33.7 mg/kg, respectively. In contrast, the culture and education zone exhibited the lowest mean content for these heavy metals at 80.1 mg/kg, 245 mg/kg, and 13.2 mg/kg, respectively. The highest (80.4 mg/kg) and lowest (70.5 mg/kg) mean concentrations of V were observed in the cultural and educational area and the commercial area. For Pb, Mn, and Ni, the mean concentrations of different functional areas were relatively constant.

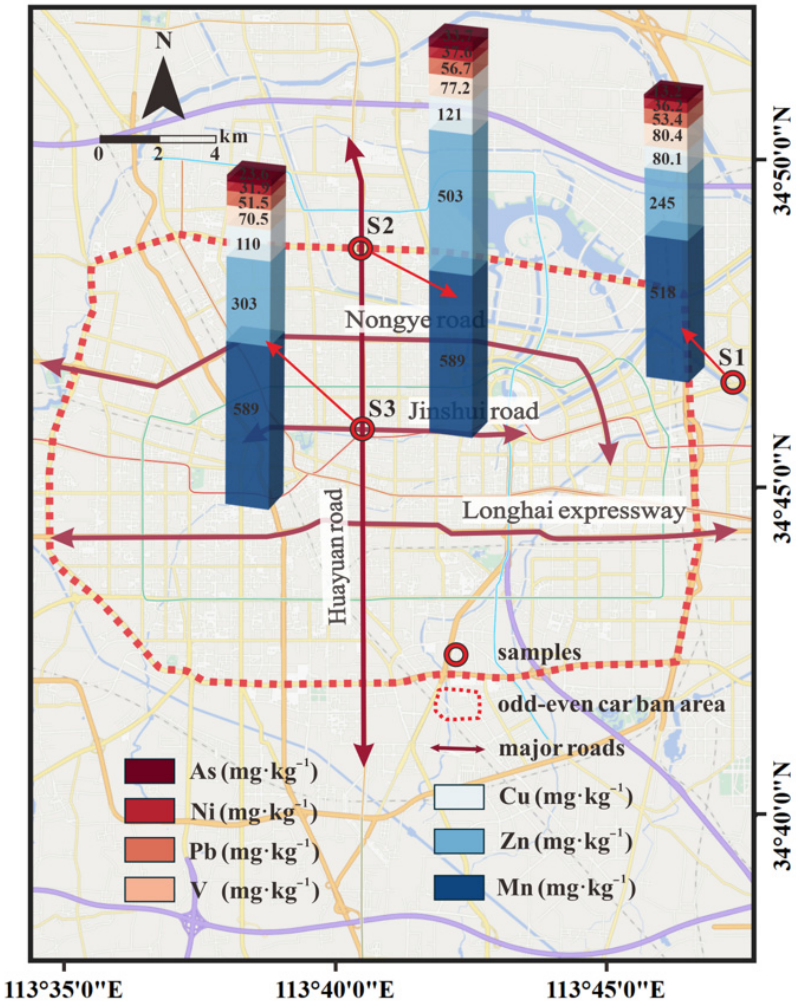


Figure 2. The distribution of mean concentrations for heavy metals in the urban street dust of Zhengzhou (mg·kg^{-1}, dry weight) from three functional areas. Note: S1, culture and education area; S2, traffic area; S3, commercial area.

The variations in heavy metal contents were mainly attributed to the distinctive surrounding environments across the three functional areas. Situated on the edge of the traffic restriction area on the northern third ring road, the traffic area is surrounded by residences, manufacturing enterprises, automotive component markets, and a coach station. The confluence of construction activities, high-density traffic, and industrial sources may contribute to heavy metal pollution in this area. The commercial area, as a central part of Zhengzhou, with residential complexes, adjacent to the Zijingshan shopping district, and with several governmental buildings, experiences elevated population density and traffic movement, potentially elevating heavy metals concentrations. Conversely, the cultural and educational area, located within Longzihu College Park and distanced from commercial and industrial activities, exhibits relatively lower concentrations of most heavy metals.

3.3. Seasonal Variations in Heavy Metal Concentrations

Heavy metal concentrations in street dust from Zhengzhou city across four seasons are presented in Figure 3. The heavy metal mean concentrations of As, Cu, and Zn exhibited significant variations across seasons whereas the seasonal variations for V, Mn, Ni, and Pb were limited, indicating a relatively constant source for these pollutes (Figure 3a). The concentrations of V, Cu, Zn, and As exhibited a similar variation, with an upward trend during fall and winter compared to spring and summer. For Mn, Ni, and Pb, the highest concentration was observed during the spring season. The seasonal variations in such heavy metals demonstrated the potential sources for the pollutes varying from spring to winter.

Seasonal trends in studied heavy metal concentrations among three functional areas are given in Figure 3b. For Mn, Ni, and Pb, their concentrations reached the highest levels in the spring and then declined notably from the summer to winter except for the cultural and education area, where Mn and Pb increased in the winter. The variations in Zn, Cu, and As exhibited similar patterns for three functional areas. The cultural and education area was less polluted for all seasons. Concentrations of Zn, Cu, and As in the traffic area were higher than in the other two areas, especially during the fall. The variation in these three metals was much different in the commercial area, which exhibited a significant increase in the winter. The mean concentrations of V were relatively constant and not significantly affected by season. However, V varied more widely in the commercial area, especially during the summer.

The elevated concentrations of heavy metals during the spring could be attributed to the prevalent dry weather in Zhengzhou, which exacerbates dust pollution. In addition, according to Wang et al. (2020) [88], localized pollutant accumulation in Zhengzhou during the spring is compounded by an influx of contaminants from upstream contaminated areas such as Hebei Province. In spite of the high temperatures in summer facilitating the erosion of metals and alloys used in car components [21,89], the rainy climate during summer leads to the migration of pollutants through surface runoff, resulting in variable but generally low concentrations of heavy metals in the street dust. During the fall, low wind speed and high atmospheric stability hinder the dispersion and dilution of pollutants in Zhengzhou, promoting the accumulation of contaminants in the local area. Moreover, Zhengzhou regularly faces pollution transported from the northern provinces, further deteriorating the city's air quality. As a result, the precipitation of suspended particles and heavy metals is more significant during the fall, increasing heavy metal contents in the road dust of Zhengzhou. The anomalous enrichment of As, Zn, and Cu in the traffic area during the fall may be related to the intensive construction of residences in this area. The heating period of Zhengzhou covered the entire winter. The increases in heavy metal contents such as V, Cu, Zn, and As during the winter were mainly attributed to combustion activities [14,28,36,37], especially for the commercial area and the culture and education area. Due to the great heating demands of these two areas, a heating station is placed in each area, contributing to the increase in heavy metals. Despite numerous residences in the traffic area, this area was not covered by municipal heating before 2010. Many earlier residences are still not

centrally heated and no heating station is present. Moreover, the industrial and constructive activities were limited during the winter of 2019 in Zhengzhou. These factors led to the descent of heavy metals in the traffic area during the winter. The mean concentrations of V were relatively constant variable and not significantly affected by season. However, V varied more widely in the commercial area, especially during the summer.

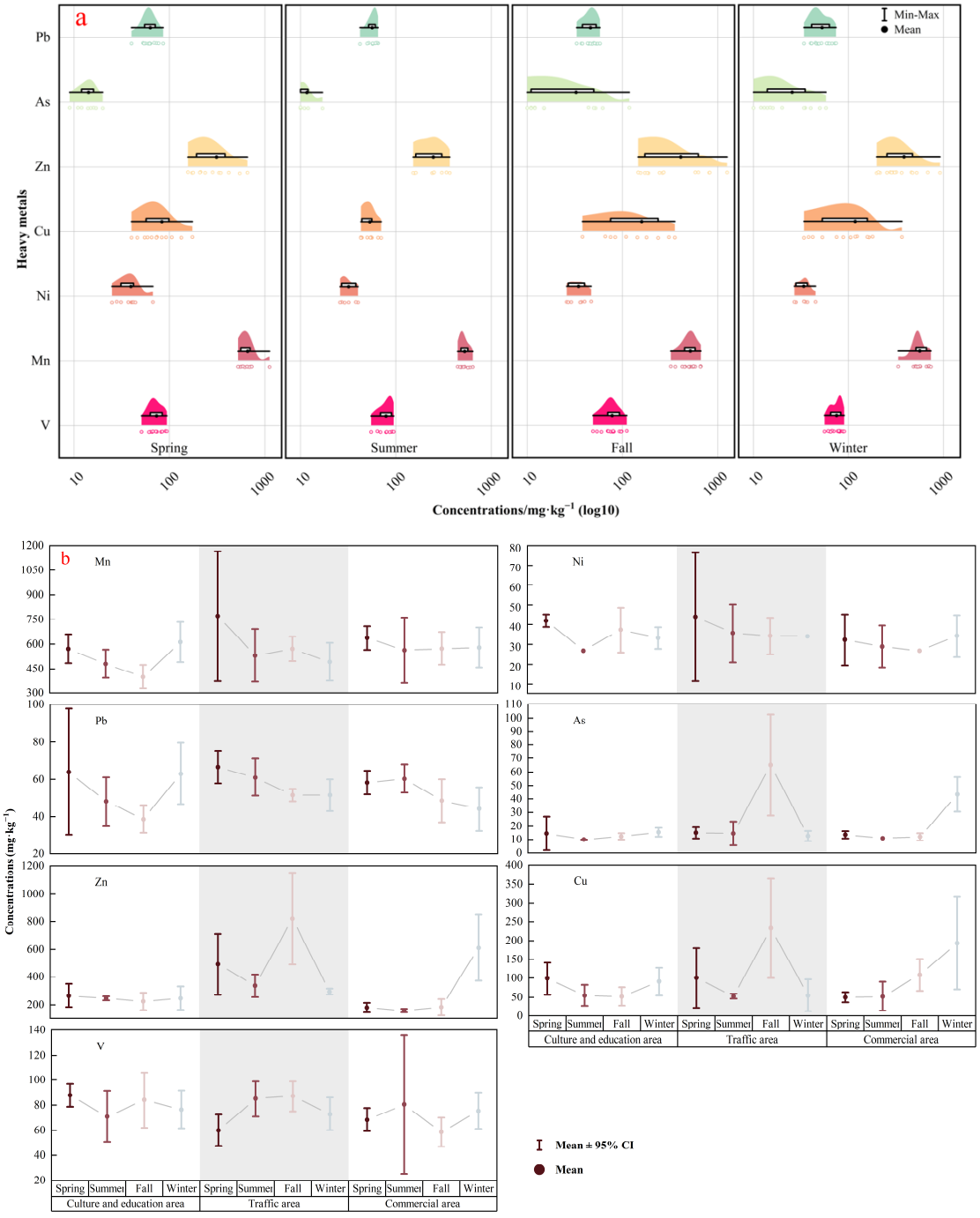


Figure 3. Seasonal variations in heavy metal concentrations. (**a**) The mean concentrations of heavy metals. (**b**) Seasonal variations in heavy metal concentrations from three functional areas. Note: (**a**) The ends of the half box represent the 25th and 75th percentile values, respectively. The horizontal line at the bottom and top denotes the minimum and maximum concentration. The data distribution is depicted by colorful dots. (**b**) Data are represented as the mean ± 95% CI (confidence interval). The solid circle represents the mean heavy metal concentrations.

3.4. Pollution Level Assessment

3.4.1. Geo-Accumulation Index (I_{geo})

The contaminated levels of heavy metals in the street dust of Zhengzhou were evaluated by I_{geo} (Figure 4). For V and Mn, the I_{geo} ranged from −0.970 to 0.209 and −0.962 to 0.838, respectively, mainly located in the uncontaminated zone. The I_{geo} of Ni (−0.333 to 1.089) was slightly higher than that of V and Mn, spanning from an uncontaminated to a moderately contaminated zone. The median value of I_{geo} for As (0.322) was similar to that of Ni (0.152), while the mean value of As (0.590) was much higher, due to the wide variation of As contents. The extreme values of I_{geo} for As are for the strongly contaminated zone. The I_{geo} varied around 1 with a mean and median values of 0.961 and 0.973, respectively. It indicated an uncontaminated to moderately contaminated level for Pb. Notably, the higher contaminated levels of Cu and Zn in Zhengzhou were demonstrated by their I_{geo} (0.695 to 4.115, 1.213 to 4.315, respectively) which were identified as strong to extreme contamination.

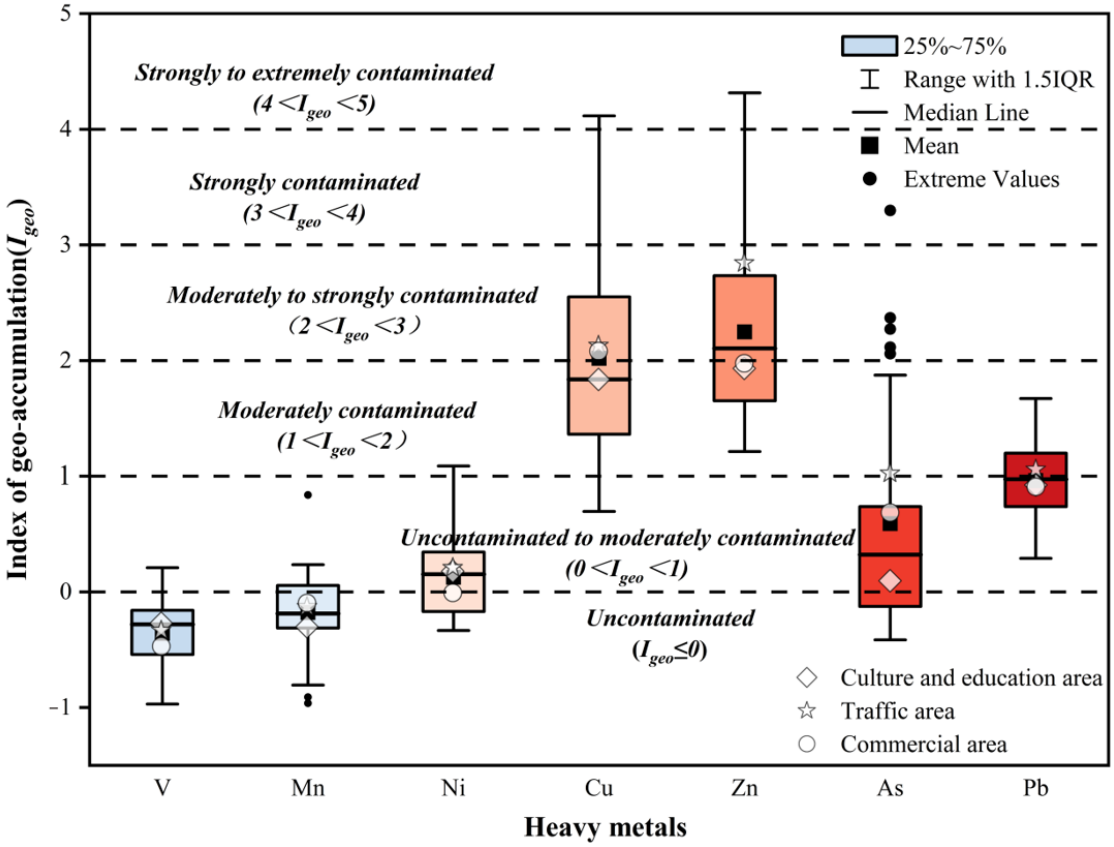


Figure 4. A box plot of the geo-accumulation index (I_{geo}) for selected heavy metals in urban road dust. Note: The dashed line denotes the threshold of contamination assessment and their classification values are listed in Table S1. The black horizontal line in the middle of the box represents the median values, while the solid black square in the box represents the mean values. The ends of the box represent the 25th and 75th percentile values, respectively. The horizontal line in the bottom and top of the box plots denotes a multiplication of the interquartile range (IQR) by 1.5.

Regarding the three functional areas, the mean I_{geo} values for most heavy metals in the traffic area were higher than the other two areas, especially for Zn and As, indicating higher contamination levels. The mean values of I_{geo} for V and Mn were all below 0, indicating the uncontaminated level. The mean I_{geo} values for Ni and Pb in the three areas showed limited variation, demonstrating the uncontaminated to moderately contaminated level. The mean values of I_{geo} for Cu, Zn, and As all followed the sequence: traffic area > com-

mercial area > cultural and educational area, ranging from uncontaminated to moderately contaminated up to moderately to strongly contaminated levels.

3.4.2. Evaluation of Potential Ecological Risk

Taking the background soil value for Zhengzhou city as the reference value, the potential ecological risks of heavy metals in street dust from three functional areas were evaluated with Hakanson's approach [53]. The calculation method is detailed in Section 2.3 and the categories are listed in Table S2.

Overall, the comprehensive potential ecological risk index (RI) in the study region, with the ranking of traffic area > commercial area > culture and education area, mainly fell within the moderate ecological risk category. For the individual potential ecological risk factor (Er^i), the values of V, Mn, Zn, Pb, and Ni for three functional areas were all below 40, implying low potential ecological risks (Table 2). But the Er^i values for Cu and As were higher than for other elements, especially in the traffic area, where those mean values yielded 43.4 and 42.1 for Cu and As, respectively. This indicates moderate ecological risks for these two pollutes. Notably, the Er^i values of As and Cu in the traffic area during the fall exceeded 80, with values of 82.94 and 81.5, respectively, representing considerable ecological risks. In the commercial area, the values of Er^i for As (54.3) and Cu (69.3) during the winter were within the moderate ecological risk level. Arsenic is strongly biotoxic, carcinogenic, teratogenic, and mutagenic [14]. Cu, despite its essential metabolic role, poses a risk to liver health when excessively present in the environment or body [90]. Therefore, Cu and As should be placed on high alert as ecological hazards and be considered as the primary control heavy metals.

Table 2. Results of potential ecological risk assessment for heavy metals in urban street dusts.

Functional Areas	Seasons	Er^i							RI
		V	Mn	Cu	Zn	As	Pb	Ni	
Culture and education area (S1)									
	Spring (n = 4)	2.74	1.37	35.36	6.33	18.15	17.78	10.00	91.73
	Summer (n = 3)	2.22	1.15	19.52	5.87	12.50	13.33	6.45	61.05
	Fall (n = 5)	2.62	0.96	18.55	5.34	15.35	10.72	8.88	62.43
	Winter (n = 5)	2.40	1.47	32.66	5.88	19.28	17.50	7.93	87.11
	Mean (n = 17)	2.51	1.24	28.60	5.82	16.54	14.84	8.62	78.17
Traffic area (S2)									
	Spring (n = 4)	1.87	1.85	36.06	11.69	18.77	18.46	10.47	99.17
	Summer (n = 3)	2.65	1.28	18.93	8.01	18.15	16.95	8.48	74.45
	Fall (n = 5)	2.72	1.37	**82.94**	19.51	**81.50**	14.28	8.17	**210.49**
	Winter (n = 5)	2.28	1.18	19.55	7.03	15.83	14.28	8.10	68.26
	Mean (n = 17)	2.41	1.41	43.37	11.97	42.12	15.74	8.95	125.97
Commercial area (S3)									
	Spring (n = 4)	2.15	1.53	17.86	4.25	16.90	16.18	7.70	66.56
	Summer (n = 3)	2.52	1.35	18.68	3.74	13.80	16.77	6.90	63.76
	Fall (n = 5)	1.83	1.38	38.93	4.33	15.03	13.44	6.45	81.39
	Winter (n = 5)	2.36	1.39	**69.29**	14.54	**54.26**	12.23	8.15	**162.23**
	Mean (n = 17)	2.21	1.41	39.38	7.21	29.49	14.31	7.60	101.61

Note: single potential ecological risk factor (Er^i > 80) and comprehensive potential ecological risk (RI > 100) are marked in bold.

3.5. Health Risk Assessment

3.5.1. Non-Carcinogenic Risk

Table 3 presents the non-carcinogenic risk results for V, Mn, Cu, Zn, As, Pb, and Ni among children and adults via three exposure pathways (hand-to-mouth ingestion, inhalation, and dermal contact). The HI values for adults were all below 1, indicating negligible non-carcinogenic risks. For children, the HI values of heavy metals also yielded negligible risks, except for As. The high HI values of As in the traffic (1.73E+00) and

commercial areas (1.21E+00) for children were mainly attributed to the high HQ values through ingestion in these two functional areas (1.44E+00 and 1.00E+00, respectively), suggesting potential non-carcinogenic risks. For different ways of exposure, the HQ values through inhalation were significantly lower than those of hand-to-mouth ingestion and dermal contact. These results suggested greater health impacts of heavy metals in road dust on children compared to adults, especially for As which can be toxic even at low concentrations [14]. Due to behaviors such as finger biting and finger sucking [25,91], children are more prone to ingesting dust particles than adults [92], which could be absorbed rapidly [17]. Consequently, residents chronically exposed to commercial and traffic environments, particularly children, are more vulnerable to non-carcinogenic risks of heavy metals.

Table 3. Non-carcinogenic risk and carcinogenic risk results for children and adults.

Metal			V	Mn	Cu	Zn	As	Pb	Ni
Noncarcinoge-nic risks	Children								
	HQ_{ing}	S1	1.47E−01	1.44E−01	2.56E−02	1.04E−02	5.63E−01	1.95E−01	2.31E−02
		S2	1.41E−01	1.64E−01	3.88E−02	2.14E−02	**1.44E+00**	2.07E−01	2.40E−02
		S3	1.29E−01	1.64E−01	3.52E−02	1.29E−02	**1.00E+00**	1.88E−01	2.04E−02
	HQ_{inh}	S1	4.05E−06	1.28E−02	7.06E−07	2.87E−07	3.79E−05	5.35E−06	6.19E−07
		S2	3.89E−06	1.45E−02	1.07E−06	5.91E−07	9.66E−05	5.67E−06	6.43E−07
		S3	3.55E−06	1.45E−02	9.72E−07	3.56E−07	6.76E−05	5.16E−06	5.46E−07
	HQ_{dermal}	S1	4.11E−01	1.01E−01	2.39E−03	1.46E−04	1.15E−01	3.64E−02	2.40E−03
		S2	3.95E−01	1.15E−01	3.62E−03	3.00E−04	2.94E−01	3.86E−02	2.49E−03
		S3	3.61E−01	1.15E−01	3.29E−03	1.81E−04	2.06E−01	3.51E−02	2.11E−03
	HI	S1	5.58E−01	2.57E−01	2.80E−02	1.06E−02	6.79E−01	2.32E−01	2.55E−02
		S2	5.36E−01	2.93E−01	4.24E−02	2.17E−02	**1.73E+00**	2.46E−01	2.65E−02
		S3	4.89E−01	2.93E−01	3.85E−02	1.31E−02	**1.21E+00**	2.23E−01	2.25E−02
	Adults								
	HQ_{ing}	S1	1.57E−02	1.54E−02	2.74E−03	1.12E−03	6.03E−02	2.09E−02	2.48E−03
		S2	1.51E−02	1.75E−02	4.16E−03	2.30E−03	1.54E−01	2.22E−02	2.58E−03
		S3	1.38E−02	1.75E−02	3.78E−03	1.38E−03	1.08E−01	2.02E−02	2.18E−03
	HQ_{inh}	S1	1.68E−06	5.29E−03	2.92E−07	1.19E−07	1.57E−05	2.22E−06	2.57E−07
		S2	1.61E−06	6.01E−03	4.43E−07	2.45E−07	4.00E−05	2.35E−06	2.67E−07
		S3	1.47E−06	6.02E−03	4.03E−07	1.47E−07	2.80E−05	2.14E−06	2.26E−07
	HQ_{dermal}	S1	6.28E−02	1.54E−02	3.65E−04	2.23E−05	1.76E−02	5.56E−03	3.66E−04
		S2	6.03E−02	1.75E−02	5.53E−04	4.58E−05	4.49E−02	5.90E−03	3.81E−04
		S3	5.50E−02	1.75E−02	5.02E−04	2.76E−05	3.14E−02	5.36E−03	3.23E−04
	HI	S1	7.85E−02	3.61E−02	3.11E−03	1.14E−03	7.80E−02	2.65E−02	2.84E−03
		S2	7.54E−02	4.10E−02	4.71E−03	2.34E−03	1.99E−01	2.81E−02	2.96E−03
		S3	6.88E−02	4.10E−02	4.28E−03	1.41E−03	1.39E−01	2.55E−02	2.51E−03
Carcinogenic risks	$LADD_{inh}$	S1					1.06E−09		2.91E−09
		S2					2.71E−09		3.02E−09
		S3					1.89E−09		2.56E−09
	CR_{inh}	S1					1.60E−08		2.44E−09
		S2					4.08E−08		2.54E−09
		S3					2.86E−08		2.15E−09

Note: hazard quotient (HQ > 1) and hazard index (HI > 1) are marked in bold.

3.5.2. Carcinogenic Risk

The carcinogenic risks through inhalation for Ni and As in three functional zones were shown and presented in Table 3. The CR_{inh} values of Ni in the cultural and educational areas, traffic areas, and commercial areas are 2.44E−09, 2.54E−09, and 2.15E−09, respectively. These values are below the risk threshold of 1.00E−06 recommended by the U.S. Environmental Protection Agency [58], indicating negligible carcinogenic risks. The carcinogenic risk of As decreased in the following order: traffic area > commercial area > cultural and educational area. Despite the value for the CR_{inh} of As being one magnitude higher than

for Ni, these values also yielded negligible carcinogenic risks for As. The combustion of fossil fuels, widespread use of antiseptic products and pesticides, food, and tobacco are considered critical sources of As [14,43,66], which may be responsible for the higher carcinogenicity values of As in traffic areas of Zhengzhou.

3.6. Heavy Mental Source Recognition

Pearson's correlation coefficient analysis, principal component analysis (PCA), and cluster analysis (CA) were used to discern the correlation and potential sources of heavy metals. Prior to the data analysis, a data normality test was necessary to prevent the distortion of the results arising from fundamental unit limitations and differences in the order of magnitude [23]. In this study, the initial distribution of data was non-normal, which was converted to a lognormal distribution during data normalization.

The correlation coefficient analysis is widely applied to investigate inter-element relationships, which could indicate the affiliation of their potential sources [93–95]. Pearson's correlation coefficient analysis was conducted in this study and the analytical results were depicted as a heatmap (Figure 5a). Elemental pairs, such as As-Zn (0.92), Cu-Zn (0.83), and As-Cu (0.78), exhibited significant positive correlations at the significance level of $p < 0.01$, indicating a potential common source for As, Zn, and Cu. A weakly positive correlation between Mn-Ni (0.51) and Mn-Pb (0.36) at a level of $p < 0.01$ as well as V-As (0.37) at level of $p < 0.05$ demonstrated that these metals have some relevance but could be contributed by diverse sources.

Principal component analysis (PCA) was applied for further source identification by using several principal components through dimensionality reduction. This analysis could identify and categorize principal component information based on the characteristics of elements [96]. The factor analysis method, Varimax rotation with Kaiser normalization, was applied to identify sources of heavy metals in street dust from Zhengzhou City [97]. Before analysis, the concentration of heavy metals was normalized and subjected to the KMO (Kaiser–Meyer–Olkin) and Bartlett's spherical tests. The KMO test yielded a value higher than 0.5 and Bartlett's test resulted in a value lower than 0.05, indicating that the data were suitable for further principal component analysis. Eigenvalues and eigenvectors were extracted from the correlation matrix, and the factors, variance proportion, and cumulative proportion of variance were then calculated. The results of principal component analysis (PCA) are listed in Table 4. Five components were extracted, collectively explaining 98.07% of the total variance. Among them, four principal components (PC) presented eigenvalues greater than 1: PC 1 (2.81), PC 2 (1.62), PC 3 (1.18), and PC 4 (1.04). PC 1 explains 40.19% of the total variance and presents heavy loads on Zn (0.98), Cu (0.95), and As (0.93). PC 2 consisted of Ni (loading 0.98) and Mn (loading 0.77), accounting for 23.12% of the total variance. PC 3 explains 16.82% of the total variance and is dominated by the high loading values of V (0.97) (Figure 5b). Regarding PC 4, it accounted for 14.86% of the total variance, including for Pb with a loading value of 0.98.

To validate the PCA results, cluster analysis (CA) was straightforwardly conducted with Ward's method [94]. The data should be standardized with the Z-Scores method for analytical preparation. The results were presented as Euclidean distance [78]. Individuals with different levels of similar traits clustered as one category at different Euclidean distances. A shorter Euclidean distance indicated higher similarity between individuals. In this study, the heavy metals clustered into four groups: (1) Cu, Zn, and As; (2) V; (3) Mn and Ni; and (4) Pb (Figure 5c). This result was consistent with that of PCA.

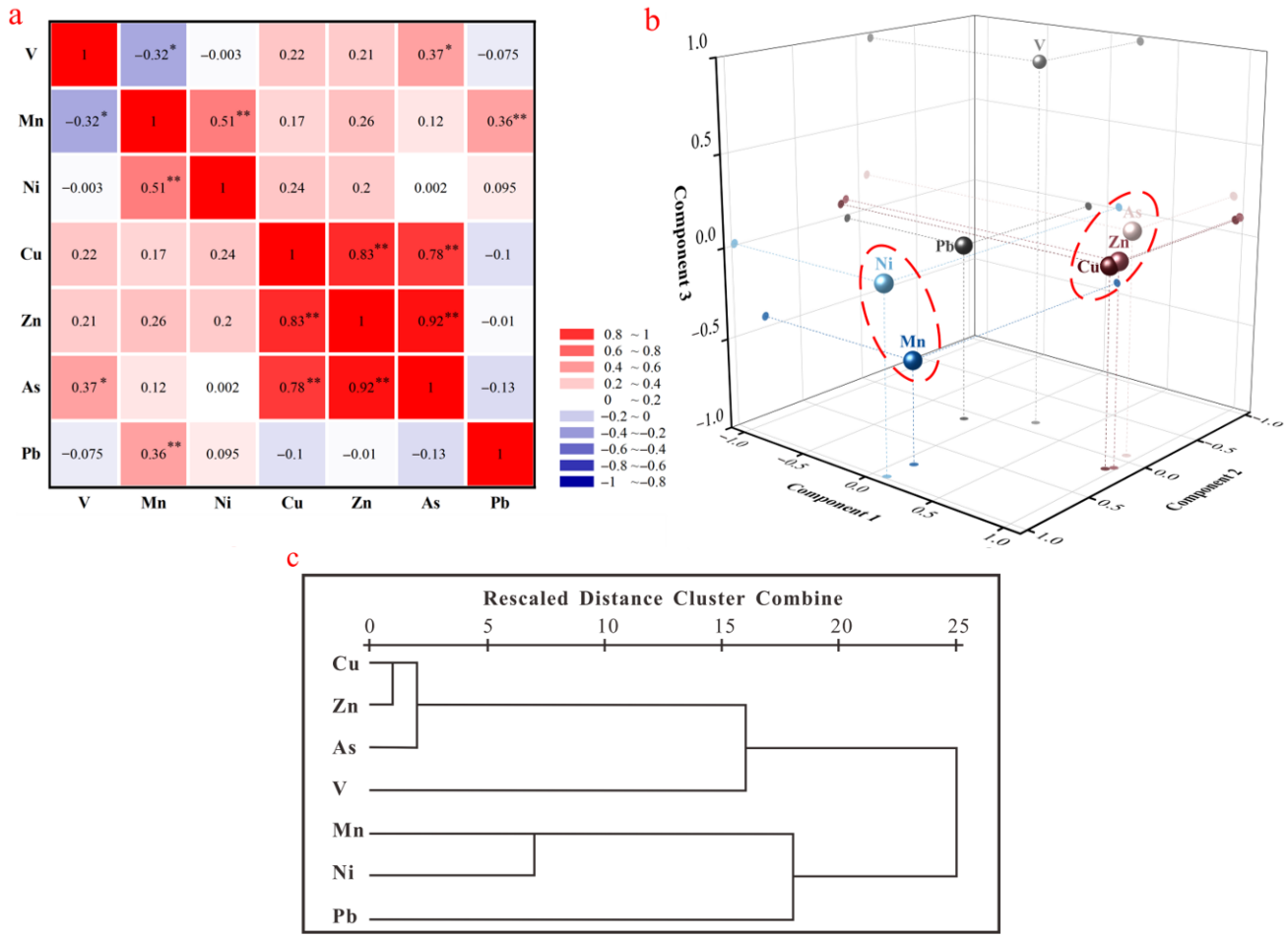


Figure 5. A source analysis of heavy metal contamination in urban street dust. (**a**) A heatmap illustrating the Pearson correlation coefficients of heavy metals. (**b**) Diagrams of three-dimensional space: three principal components for seven heavy metals in Zhengzhou. (**c**) The results of the cluster analysis of heavy metals obtained by Ward's hierarchical clustering method (the distances reflect the degree of correlation between different elements). Note: (**a**) one (*) and two (**) asterisks indicate that the correlation is significant at the 0.05 level (two-tailed) and the 0.01 level (two-tailed), respectively. The values of correlation coefficients have been labeled in the figure.

Table 4. Principal rotated component matrix for data of street dust in Zhengzhou.

Metals	Components				
	1	**2**	**3**	**4**	**5**
Zn	**0.98**	0.11	0.09	−0.05	0.03
Cu	**0.95**	0.15	0.07	−0.07	−0.17
As	**0.93**	−0.07	0.20	−0.15	0.17
Ni	0.09	**0.98**	0.01	0.03	−0.11
Mn	0.09	**0.77**	−0.44	0.21	0.38
V	0.22	−0.12	**0.97**	−0.01	−0.02
Pb	−0.15	0.10	−0.02	**0.98**	0.02
Eigenvalues	2.81	1.62	1.18	1.04	0.22
Variance percentage (%)	40.19	23.12	16.82	14.86	3.08
Cumulative variance (%)	40.19	63.31	80.13	94.99	98.07

Note: significant loading factors (>0.7) are marked in bold. Extraction method: principal component analysis. Rotation method: varimax with Kaiser normalization. Rotation converged in five iterations.

With the discussions above, the potential sources of heavy metal in road dust of Zhengzhou were identified. Zn, Cu, and As were strongly correlated in both correlation

coefficient analysis and PCA and classified together in CA (Figure 5 and Table 4), showing a potential common source. The concentrations of these three heavy metals were more than two times higher than Zhengzhou's soil background values, with their high I_{geo} and RI values (Figure 4 and Table 2), demonstrating clear signs of anthropogenic influence. According to previous studies, As serves as a tracer element for coal combustion [98], whereas Zn and Cu originate from sources such as tire abrasion, the corrosion of vehicles, lubricant leaks, traffic emissions, coal combustion, and industrial emissions from incinerators [84,98–100]. Spatially, these elements were more enriched in traffic and commercial areas in Zhengzhou, indicating that Cu, Zn, and As in road dust mainly originates from traffic activities [7,16,96]. Additionally, industrial facilities such as food factories and machinery manufacturing plants near the traffic area (S2) also contributed to the accumulation of these three elements. These elements accumulate in street dust through atmospheric deposition and particle adsorption and are distinctly influenced by Zhengzhou's continental monsoon climate, which contributes to the accumulation of pollutants, particularly during the fall and winter with low humidity.

V is not strongly correlated with other studied metals and separated from other metals in PCA and CA, exhibiting a unique source (Figure 5). Fossil fuel combustion as well as catering events related to food shops and restaurants were identified as potential sources of V [8,14]. The spatial distribution of V across the three functional areas in Zhengzhou yielded slightly higher concentrations in the vicinity of the cultural and commercial regions, indicating that V in the road dust of Zhengzhou was mainly attributed to catering events.

For Mn and Ni, the mean concentrations slightly surpassed or were close to the background soil values in Zhengzhou (Table 1), suggesting natural sources such as crustal materials and weathered sediments [20,94,97]. However, the maximum concentrations of Mn and Ni in dust samples were 1118 mg/kg and 67 mg/kg, respectively (Table 1), both of which occurred in areas with heavy traffic. It indicated a potential influence of traffic activities on accumulations of Mn and Ni. Nickel alloy corrosion in vehicles and tailpipe emissions were the potential sources of Ni [91]. Mn mainly stemmed from tire aging and fuel additives in transportation [14,101]. Thus, they were also influenced by anthropogenic sources, particularly traffic pollution. Furthermore, the concentrations of Mn and Ni notably peaked in the spring (Figure 3) due to the dry weather causing dust pollution in Zhengzhou, along with pollutant influx from the upstream contaminated area in Hebei Province [88]. Mn and Ni can be derived from coal combustion [84], released into the air with fly ash, resuspended, and deposited on road dust. Spatial and seasonal variations in concentrations of Mn and Ni can be attributed to mixed sources. Therefore, Mn and Ni were identified as a blend of natural and traffic-related sources, supported by the significant positive correlations of Mn-Ni and Mn-Pb in the correlation analysis and PCA.

Pb is considered a trace element in gasoline combustion and is also found in gasoline leaks, exhaust fumes, brake wear, coal burning, as well as emissions from industrial processes such as cement and metallurgical [18,24,37,102] processes. The spatial and seasonal variation of Pb (Figures 2 and 3a) indicated that it mainly originated from different levels of traffic activity in Zhengzhou which had transported pollutants from upstream polluted areas. Meanwhile, multiple constructions near the traffic and cultural districts may release Pb due to the peeling of architectural paint and coatings on the building surfaces [97]. Compared with other major cities in China and overseas (Figure S1), the concentrations of Pb in Zhengzhou were relatively low, indicating the effects of the use of unleaded gasoline and the development of new energy automobiles [99].

4. Conclusions

In the present study, an investigation was conducted on the spatial and seasonal variations in concentrations, health risks, and sources of seven heavy metals present in street dust from Zhengzhou, China. The mean concentrations of the seven heavy metals exceeded their respective soil background values in Zhengzhou. In particular, the mean

levels of Zn and Cu exceeded their corresponding background values by 7.33 and 6.5 times, respectively, showing significant influences from anthropogenic activities. Spatially, total concentrations of heavy metals were found to be higher in the traffic area than in the commercial area, with the culture and education area showing the lowest levels. The concentrations of V, Cu, Zn, and As exhibited a similar variation, with an upward trend during fall and winter compared to spring and summer. For Mn, Ni, and Pb, the highest concentration was observed during the spring season. For children, the HQ values of As through ingestion in both commercial and traffic areas exceeded 1, indicating higher vulnerability to metal exposure risks compared to adults.

According to the findings, the anthropogenic sources of heavy metal contamination in street dust include industrial, traffic, and construction activities. Natural sources may be related to dust, rainfall, high temperatures, and seasonal prevailing winds. Despite Zhengzhou implementing environmental pollution control measures, including fuel substitution, centralized heating, prohibiting the manufacture and use of leaded gasoline, and the closure and renovation of coal and power plants, the cumulative effect of pollutants persists. Therefore, reducing environmental pollution in Zhengzhou requires the continued stepping up of the control of motor vehicle exhaust emissions and the promotion of the transformation of coal combustion in heat source plants.

Supplementary Materials: The following supporting information can be downloaded at https://www.mdpi.com/article/10.3390/su16177604/s1, Figure S1: Comparison of the heavy metal concentrations from different cities around the world.; Table S1: Classification criteria of geo-accumulation pollution index; Table S2: Categories of single and comprehensive potential ecological risks of heavy metal pollution; Table S3: Exposure param-eters for the health risk assessment model; Table S4: Reference dose (RfD) for non-carcinogenic metals and slope factors (SF) for carcinogenic metals with different exposure pathways [16,20,43,57,58,60,62,67,75,79–84,103–106].

Author Contributions: Methodology, M.R., Y.D., W.N., J.S., Y.T., H.W., F.Z. and X.H. (Xiaoxiao Huang); formal analysis, Y.D.; investigation, J.S., Y.T., X.H. (Xiao Han) and F.L.; writing—original draft preparation, Y.D.; writing—review and editing, M.R.; supervision, Z.H.; funding acquisition, X.H. (Xiaoxiao Huang). All authors have read and agreed to the published version of the manuscript.

Funding: This research was funded by the Natural Science Foundation of China (Grant No. 41803033, 41903034), the Key Research and Development Project of Henan Province (Grant No. 221111321500), the Key Research Project of the Higher Education Institution in Henan Province (19A170009), and the Central Plains Science and Technology Innovation Leader Project (Grant No. 214200510030).

Institutional Review Board Statement: Not applicable.

Informed Consent Statement: Not applicable.

Data Availability Statement: The data presented in this study are available in the Supplementary Materials of this article.

Acknowledgments: We are grateful to Han Song, Yue Liang, and Lili Liu for sampling, and Bolin Wang for analysis. We are grateful to the anonymous reviewers who helped improve the paper and the editors for handling, editing, and advising.

Conflicts of Interest: The authors declare no conflicts of interest.

References

1. Salim Akhter, M.; Madany, I.M. Heavy metals in street and house dust in Bahrain. *Water Air Soil Pollut.* **1993**, *66*, 111–119. [CrossRef]
2. Li, J.; Li, H.; Zang, F.; Chang, G.H.; Wang, J.H.; Li, Y.W. Contamination and risk assessment of heavy metals in ambient street dust from one petrochemical industrial base in Sichuan Basin. *Environ. Sci. Technol.* **2021**, *44*, 338–346, (In Chinese with English abstract).
3. Harrison, R.M.; Laxen, D.P.H.; Wilson, S.J. Chemical associations of lead, cadmium, copper, and zinc in street dusts and roadside soils. *Environ. Sci. Technol.* **1981**, *15*, 1378–1383. [CrossRef]
4. Zheng, N.; Liu, J.S.; Wang, Q.C.; Liang, Z.Z. Health risk assessment of heavy metal exposure to street dust in the zinc smelting district, northeast of China. *Sci. Total Environ.* **2010**, *408*, 726–733. [CrossRef] [PubMed]

5. Wang, Q.; Lu, X.; Pan, H. Analysis of heavy metals in the re-suspended road dusts from different functional areas in Xi'an, China. *Environ. Sci. Pollut. Res.* **2016**, *23*, 19838–19846. [CrossRef] [PubMed]
6. Pan, H.Y.; Lu, X.W.; Lei, K. A comprehensive analysis of heavy metals in urban road dust of Xi'an, China: Contamination, source apportionment and spatial distribution. *Sci. Total Environ.* **2017**, *609*, 1361–1369. [CrossRef] [PubMed]
7. Kabir, M.H.; Kormoker, T.; Islam, M.S.; Khan, R.; Shammi, R.S.; Tusher, T.R.; Proshad, R.; Islam, M.S.; Idris, A.M. Potentially toxic elements in street dust from an urban city of a developing country: Ecological and probabilistic health risks assessment. *Environ. Sci. Pollut. Res.* **2021**, *28*, 57126–57148. [CrossRef] [PubMed]
8. Li, F.Q.; Pan, H.M.; Ye, W.; Zhu, L.D.; Wang, Z.G. Specificity of the heavy metal pollution and the ecological hazard in urban dust. *J. Anhui Agric. Sci.* **2008**, *36*, 2495–2498, (In Chinese with English abstract).
9. Zhao, H.T.; Li, X.Y.; Yin, C.Q. Research progress on the relationship of pollutants between road-deposited sediments and its washoff. *Acta Ecol. Sinica* **2012**, *32*, 8001–8007, (In Chinese with English abstract).
10. Rahman, M.S.; Khan, M.D.H.; Jolly, Y.N.; Kabir, J.; Akter, S.; Salam, A. Assessing risk to human health for heavy metal contamination through street dust in the Southeast Asian Megacity: Dhaka, Bangladesh. *Sci. Total Environ.* **2019**, *660*, 1610–1622. [CrossRef]
11. Cai, Q.Y.; Mo, C.H.; Li, H.Q.; Lü, H.; Zeng, Q.Y.; Li, Y.W.; Wu, X.L. Heavy metal contamination of urban soils and dusts in Guangzhou, South China. *Environ. Monit. Assess.* **2013**, *185*, 1095–1106. [CrossRef] [PubMed]
12. Liang, F.; Zhang, G.L.; Tan, M.G.; Yan, C.G.; Li, X.; Li, Y.L.; Li, Y.; Zhang, Y.M.; Shan, Z.C. Lead in children's blood is mainly caused by coal-fired ash after phasing out of leaded gasoline in Shanghai. *Environ. Sci. Technol.* **2010**, *44*, 4760–4765. [CrossRef] [PubMed]
13. Cao, S.; Duan, X.; Zhao, X.; Ma, J.; Dong, T.; Huang, N.; Sun, C.; He, B.; Wei, F. Health risks from the exposure of children to As, Se, Pb and other heavy metals near the largest coking plant in China. *Sci. Total Environ.* **2014**, *472*, 1001–1009. [CrossRef]
14. Duan, J.C.; Tan, J.H. Atmospheric heavy metals and arsenic in China: Situation, sources and control policies. *Atmos. Environ.* **2013**, *74*, 93–101. [CrossRef]
15. El-Bahi, S.M.; Sroor, A.T.; Arhoma, N.F.; Darwish, S.M. XRF analysis of heavy metals for surface soil of Qarun Lake and Wadi El Rayan in Faiyum, Egypt. *Open J. Met.* **2013**, *3*, 21–25. [CrossRef]
16. Mostafa, M.T.; El-Nady, H.; Gomaa, R.M.; Abdelgawad, H.F.; Abdelhafiz, M.A.; Salman, S.A.E.; Khalifa, I.H. Urban geochemistry of heavy metals in road dust from Cairo megacity, Egypt: Enrichment, sources, contamination, and health risks. *Environ. Earth Sci.* **2023**, *83*, 37. [CrossRef]
17. Chisolm, J.; O'hara, D. Lead absorption in children: Management, clinical and environmental aspects. *Am. J. Dis. Child.* **1983**, *137*, 300.
18. Lanphear, B.P.; Roghmann, K.J. Pathways of lead exposure in urban children. *Environ. Res.* **1997**, *74*, 67–73. [CrossRef]
19. Krishna, A.K.; Mohan, K.R. Distribution, correlation, ecological and health risk assessment of heavy metal contamination in surface soils around an industrial area, Hyderabad, India. *Environ. Earth Sci.* **2016**, *75*, 411. [CrossRef]
20. Yin, R.; Wang, D.; Deng, H.; Shi, R.; Chen, Z. Heavy Metal Contamination and Assessment of Roadside and Foliar Dust along the Outer-Ring Highway of Shanghai, China. *J. Environ. Qual.* **2013**, *42*, 1724–1732. [CrossRef] [PubMed]
21. Wang, Y.P.; Qian, P.; Li, D.M.; Chen, H.F.; Zhou, X.Q. Assessing risk to human health for heavy metal contamination from public point utility through ground dust: A case study in Nantong, China. *Environ. Sci. Pollut. Res.* **2021**, *28*, 67234–67247. [CrossRef] [PubMed]
22. Gan, H.Y.; Zhuo, M.N.; Li, D.Q.; Zhou, Y.Z. Quality characterization and impact assessment of highway runoff in urban and rural area of Guangzhou, China. *Environ. Monit. Assess.* **2008**, *140*, 147–159. [CrossRef] [PubMed]
23. Zgłobicki, W.; Telecka, M.; Skupiński, S.; Pasierbińska, A.; Kozieł, M. Assessment of heavy metal contamination levels of street dust in the city of Lublin, E Poland. *Environ. Earth Sci.* **2018**, *77*, 774. [CrossRef]
24. Day, J.P.; Hart, M.; Robinson, M.S. Lead in urban street dust. *Nature* **1975**, *253*, 343–345. [CrossRef]
25. Roels, H.A.; Buchet, J.P.; Lauwerys, R.R.; Bruaux, P.; Claeys-Thoreau, F.; Lafontaine, A.; Verduyn, G. Exposure to lead by the oral and the pulmonary routes of children living in the vicinity of a primary lead smelter. *Environ. Res.* **1980**, *22*, 81–94. [CrossRef] [PubMed]
26. Dong, A.; Chesters, G.; Simsiman, G.V. Metal composition of soil, sediments, and urban dust and dirt samples from the menomonee river watershed, Wisconsin, U.S.A. *Water Air Soil Pollut.* **1984**, *22*, 257–275. [CrossRef]
27. Veron, A.; Church, T.M.; Patterson, C.C.; Erel, Y.; Merrill, J.T. Continental origin and industrial sources of trace metals in the Northwest Atlantic troposphere. *J. Atmos. Chem.* **1992**, *14*, 339–351. [CrossRef]
28. Zhu, X.; Yu, W.; Li, F.; Liu, C.; Ma, J.; Yan, J.; Wang, Y.; Tian, R. Spatio-temporal distribution and source identification of heavy metals in particle size fractions of road dust from a typical industrial district. *Sci. Total Environ.* **2021**, *780*, 146357. [CrossRef]
29. Han, Q.; Wang, M.Y.; Xu, X.H.; Li, M.F.; Liu, Y.; Zhang, C.H.; Li, S.H.; Wang, M.S. Health risk assessment of heavy metals in road dust from the fourth-tier industrial city in central China based on Monte Carlo simulation and bioaccessibility. *Ecotoxicol. Environ. Saf.* **2023**, *252*, 114627. [CrossRef] [PubMed]
30. Han, Y.M.; Du, P.X.; Cao, J.J.; Posmentier, E.S. Multivariate analysis of heavy metal contamination in urban dusts of Xi'an, central China. *Sci. Total Environ.* **2006**, *355*, 176–186.

31. Tong, S.M.; Li, H.R.; Wang, L.; Tudi, M.; Yang, L.S. Concentration, Spatial distribution, contamination degree and human health risk assessment of heavy metals in urban soils across China between 2003 and 2019-a systematic review. *Int. J. Environ. Res. Public Health* **2020**, *17*, 3099. [CrossRef]
32. Al-Khashman, O.A. Heavy metal distribution in dust, street dust and soils from the work place in Karak industrial estate, Jordan. *Atmos. Environ.* **2004**, *38*, 6803–6812. [CrossRef]
33. Adamiec, E.; Jarosz-Krzemińska, E. Human health risk assessment associated with contaminants in the finest fraction of sidewalk dust collected in proximity to trafficked roads. *Sci. Rep.* **2019**, *9*, 16364. [CrossRef]
34. Elwood, P.C. The sources of lead in blood: A critical review. *Sci. Total Environ.* **1986**, *52*, 1–23. [CrossRef] [PubMed]
35. Watt, J.; Thornton, I.; Cotter-Howells, J. Physical evidence suggesting the transfer of soil Pb into young children via hand-to-mouth activity. *Appl. Geochem.* **1993**, *8*, 269–272. [CrossRef]
36. Škrbić, B.D.; Buljovčić, M.; Jovanović, G.; Antić, I. Seasonal, spatial variations and risk assessment of heavy elements in street dust from Novi Sad, Serbia. *Chemosphere* **2018**, *205*, 452–462. [CrossRef]
37. Duan, J.; Tan, J.; Wang, S.; Hao, J.; Chai, F. Size distributions and sources of elements in particulate matter at curbside, urban and rural sites in Beijing. *J. Environ. Sci.* **2012**, *24*, 87–94. [CrossRef]
38. Ihedioha, J.N.; Ukoha, P.O.; Ekere, N.R. Ecological and human health risk assessment of heavy metal contamination in soil of a municipal solid waste dump in Uyo, Nigeria. *Environ. Geochem. Health* **2017**, *39*, 497–515. [CrossRef] [PubMed]
39. Atiemo, M.S.; Ofosu, G.; Kuranchie-Mensah, H.; Osei Tutu, A.; Linda Palm, N.D.M.; Blankson, S.A. Contamination assessment of heavy metals in road dust from selected roads in Accra, Ghana. *Res. J. Environ. Earth Sci.* **2011**, *3*, 473–480.
40. Tan, J.H.; Duan, J.C.; Ma, Y.L.; Yang, F.M.; Cheng, Y.; He, K.B.; Yu, Y.C.; Wang, J.W. Source of atmospheric heavy metals in winter in Foshan, China. *Sci. Total Environ.* **2014**, *493*, 262–270. [CrossRef] [PubMed]
41. Shen, C.Y. Pollution Characteristics of Heavy Metals in Near-Surface Dust and Risk Assessment of Human Health in Zhengzhou, China. Master's Thesis, Zhengzhou University, Zhengzhou, China, 2021.
42. Zhengzhou Bureau of Statistics. Available online: https://tjj.zhengzhou.gov.cn/tjgb/4430813.jhtml (accessed on 20 May 2024).
43. Faisal, M.; Wu, Z.N.; Wang, H.L.; Hussain, Z.; Azam, M.I. Human health risk assessment of heavy metals in the urban road dust of Zhengzhou metropolis, China. *Atmosphere* **2021**, *12*, 1213. [CrossRef]
44. Idris, A.M.; Alqahtani, F.M.S.; Said, T.O.; Fawy, K.F. Contamination level and risk assessment of heavy metal deposited in street dusts in Khamees-Mushait city, Saudi Arabia. *Hum. Ecol. Risk Assess. Int. J.* **2018**, *26*, 495–511. [CrossRef]
45. Jehan, S.; Khattak, S.A.; Muhammad, S.; Ahmad, R.; Farooq, M.; Khan, S.; Khan, A.; Ali, L. Ecological and health risk assessment of heavy metals in the Hattar industrial estate, Pakistan. *Toxin Rev.* **2020**, *39*, 68–77. [CrossRef]
46. Frydrych, A.; Jurowski, K. Portable X-ray fluorescence (pXRF) as a powerful and trending analytical tool for in situ food samples analysis: A comprehensive review of application—State of the art. *Trends Anal. Chem.* **2023**, *166*, 117165. [CrossRef]
47. Palmer, P.T.; Jacobs, R.; Baker, P.E.; Ferguson, K.; Webber, S. Use of field-portable XRF analyzers for rapid screening of toxic elements in FDA-regulated products. *J. Agric. Food Chem.* **2009**, *57*, 2605–2613. [CrossRef] [PubMed]
48. Muller, G. Index of geoaccumulation in sediments of the rhine river. *GeoJournal* **1969**, *2*, 107–126.
49. Förstner, U.; Ahlf, W.; Calmano, W.; Kersten, M. Sediment criteria development: Contributions from environmental geochemistry to water quality management. In *Sediments and Environmental Geochemistry: Selected Aspects and Case Histories*; Springer: Berlin/Heidelberg, Germany, 1990; pp. 311–338.
50. Tao, H.; Zhang, X.H.; Wang, Y.J.; Tao, E.Z.; Wang, F. Pollution characteristics and health risk assessment of heavy metals of surface dust in urban areas of Yinchuan. *Environ. Chem.* **2022**, *41*, 2573–2585, (In Chinese with English abstract).
51. Ekoa Bessa, A.Z.; Ambassa Bela, V.; Ngueutchoua, G.; El-Amier, Y.; Kamani, F.; Zebaze, L.N.; Kamguem Fotso, C.A.; Njong, V.N.; Kemgang Ghomsi, F.E.; Valipour, M.; et al. Characteristics and source identification of environmental trace metals in beach sediments along the littoral zone of Cameroon. *Earth Syst. Environ.* **2022**, *6*, 175–187. [CrossRef]
52. Cheng, H.X.; Li, K.; Li, M.; Yang, K.; Liu, F.; Cheng, X.M. Geochemical background and baseline value of chemical elements in urban soil in China. *Earth Sci. Front.* **2014**, *21*, 265–306.
53. Hakanson, L. An ecological risk index for aquatic pollution control. A sedimentological approach. *Water Res.* **1980**, *14*, 975–1001. [CrossRef]
54. Kusin, F.M.; Abd Rahman, M.S.; Madzin, Z.; Jusop, S.; Mohamat-Yusuff, F.; Ariffin, M.; Md Z, M.S. The occurrence and potential ecological risk assessment of bauxite mine-impacted water and sediments in Kuantan, Pahang, Malaysia. *Environ. Sci. Pollut. Res.* **2017**, *24*, 1306–1321. [CrossRef] [PubMed]
55. Trujillo-Gonzalez, J.M.; Torres-Mora, M.A.; Keesstra, S.; Brevik, E.C.; Jiménez-Ballesta, R. Heavy metal accumulation related to population density in road dust samples taken from urban sites under different land uses. *Sci. Total Environ.* **2016**, *553*, 636–642. [CrossRef]
56. Chen, H.; Chen, Z.B.; Chen, Z.Q.; Ou, X.; Chen, J. Calculation of toxicity coefficient of potential ecological risk assessment of rare earth elements. *Bull. Environ. Contam. Toxicol.* **2020**, *104*, 582–587. [CrossRef] [PubMed]
57. Mirzaei Aminiyan, M.; Baalousha, M.; Mousavi, R.; Mirzaei Aminiyan, F.; Hosseini, H.; Heydariyan, A. The ecological risk, source identification, and pollution assessment of heavy metals in road dust: A case study in Rafsanjan, SE Iran. *Environ. Sci. Pollut. Res.* **2018**, *25*, 13382–13395. [CrossRef] [PubMed]
58. US EPA. *Risk Assessment Guidance for Superfund*; Volume I: Human health evaluation manual (Part A), EPA/540/1-89/002; Office of Emergency and Remedial Response, U.S. Environmental Protection Agency: Washington, DC, USA, 1989.

59. US EPA. *Exposure Factors Handbook*; Office of Research and Development, National Center for Environmental Assessment, U.S. Environmental Protection Agency: Washington, DC, USA, 1997.
60. US EPA. *Supplemental Guidance for Developing Soil Screening Levels for Superfund Sites*; OSWER 9355.4-24; Office of Emergency and Remedial Response, U.S. Environmental Protection Agency: Washington, DC, USA, 2002.
61. Bartholomew, C.J.; Li, N.; Li, Y.; Dai, W.S.; Nibagwire, D.; Guo, T. Characteristics and health risk assessment of heavy metals in street dust for children in Jinhua, China. *Environ. Sci. Pollut. Res.* **2020**, *27*, 5042–5055. [CrossRef]
62. Ferreira-Baptista, L.; Miguel, E.D. Geochemistry and risk assessment of street dust in Luanda, Angola: A tropical urban environment. *Atmos. Environ.* **2005**, *39*, 4501–4512. [CrossRef]
63. Zhang, W.J.; Wang, L.J.; Wang, L.; Shi, X.M.; Lu, X.W. Assessment of pollution level and health risks of heavy metals in surface dust in Xi'an City, NW China. *Chin. J. Soil Sci.* **2017**, *48*, 481–487, (In Chinese with English abstract).
64. Shen, M.H.; Sun, L.F.; Zhang, Y.J.; Xu, X.P.; Wang, S.T.; Wu, P.P.; Yang, Y.Y.; Cao, Z.G.; Yan, G.X. Pollution characteristics of heavy metals in road dust in several cities of Henan Province. *Environ. Sci. Technol.* **2018**, *41*, 117–123, (In Chinese with English abstract).
65. Li, Z.G.; Feng, X.B.; Li, G.H.; Bi, X.Y.; Zhu, J.M.; Qin, H.B.; Dai, Z.H.; Liu, J.L.; Li, Q.H.; Sun, G.Y. Distributions, sources and pollution status of 17 trace metal/metalloids in the street dust of a heavily industrialized city of central China. *Environ. Pollut.* **2013**, *182*, 408–416. [CrossRef] [PubMed]
66. Cai, L.M.; Wang, Q.S.; Luo, J.; Chen, L.G.; Zhu, R.L.; Wang, S.; Tang, C.H. Heavy metal contamination and health risk assessment for children near a large Cu-smelter in central China. *Sci. Total Environ.* **2019**, *650*, 725–733. [CrossRef]
67. US EPA. *Supplemental Guidance for Developing Soil Screening Levels for Superfund Sites*; OSWER 9355.4-24; Office of Emergency and Remedial Response, U.S. Environmental Protection Agency: Washington, DC, USA, 2001.
68. Chang, S.L.; Ye, Z.X. The pollution state and health risk assessment of heavy metals in road dust of Chengdu. *Environ. Monit. China* **2014**, *30*, 70–75, (In Chinese with English abstract).
69. Wei, X.; Gao, B.; Wang, P.; Zhou, H.D.; Lu, J. Pollution characteristics and health risk assessment of heavy metals in street dusts from different functional areas in Beijing, China. *Ecotoxicol. Environ. Saf.* **2015**, *112*, 186–192. [CrossRef] [PubMed]
70. Chen, Y.; Sun, L.; Yun, Z.L.; Wu, G.N.; Xu, H.Y.; Chen, A.X. Heavy metal pollution of the urban street dust and health risk assessment in Xi'an. *J. Saf. Environ.* **2016**, *16*, 370–376, (In Chinese with English abstract).
71. Adimalla, N.; Wang, H.K. Distribution, contamination, and health risk assessment of heavy metals in surface soils from northern Telangana, India. *Arab. J. Geosci.* **2018**, *11*, 684. [CrossRef]
72. Tang, Z.W.; Chai, M.; Cheng, J.L.; Jin, J.; Yang, Y.F.; Nie, Z.Q.; Huang, Q.F.; Li, Y.H. Contamination and health risks of heavy metals in street dust from a coal-mining city in eastern China. *Ecotoxicol. Environ. Saf.* **2017**, *138*, 83–91. [CrossRef] [PubMed]
73. US EPA. *Risk Assessment Guidance for Superfund (RAGS)*; Volume I: Human Health Evaluation Manual; EPA/540/1-89/002; U.S. Environmental Protection Agency: Washington, DC, USA, 2011.
74. Mohmand, J.; Eqani, S.A.M.A.S.; Fasola, M.; Alamdar, A.; Mustafa, I.; Ali, N.; Liu, L.P.; Peng, S.Y.; Shen, H.Q. Human exposure to toxic metals via contaminated dust: Bio-accumulation trends and their potential risk estimation. *Chemosphere* **2015**, *132*, 142–151. [CrossRef] [PubMed]
75. Rahman, M.S.; Kumar, P.; Ullah, M.; Jolly, Y.N.; Akhter, S.; Kabir, J.; Begum, B.A.; Salam, A. Elemental analysis in surface soil and dust of roadside academic institutions in Dhaka city, Bangladesh and their impact on human health. *Environ. Chem. Ecotoxicol.* **2021**, *3*, 197–208. [CrossRef]
76. Li, H.H.; Chen, L.J.; Yu, L.; Guo, Z.B.; Shan, C.Q.; Lin, J.Q.; Gu, Y.G.; Yang, Z.B.; Yang, Y.X.; Shao, J.R.; et al. Pollution characteristics and risk assessment of human exposure to oral bioaccessibility of heavy metals via urban street dusts from different functional areas in Chengdu, China. *Sci. Total Environ.* **2017**, *586*, 1076–1084. [CrossRef] [PubMed]
77. US EPA. *Guidelines for Carcinogen Risk Assessment*; EPA/630/P-03/001F; Risk Assessment Forum, U.S. Environmental Protection Agency: Washington, DC, USA, 2005.
78. Shi, X.; Chen, L.; Wang, J. Multivariate analysis of heavy metal pollution in street dusts of Xianyang city, NW China. *Environ. Earth Sci.* **2013**, *69*, 1973–1979. [CrossRef]
79. Choi, J.Y.; Jeong, H.; Choi, K.Y.; Hong, G.H.; Yang, D.B.; Kim, K.; Ra, K. Source identification and implications of heavy metals in urban roads for the coastal pollution in a beach town, Busan, Korea. *Mar. Pollut. Bull.* **2020**, *16*, 111724. [CrossRef]
80. Aguilera, A.; Bautista, F.; Gutiérrez-Ruiz, M.; Ceniceros-Gómez, A.E.; Cejudo, R.; Goguitchaichvili, A. Heavy metal pollution of street dust in the largest city of Mexico, sources and health risk assessment. *Environ. Monit. Assess.* **2021**, *193*, 193. [CrossRef]
81. Crosby, C.J.; Fullen, M.A.; Booth, C.A.; Searle, D.E. A dynamic approach to urban road deposited sediment pollution monitoring (Marylebone Road, London, UK). *J. Appl. Geophys.* **2014**, *105*, 10–20. [CrossRef]
82. Huang, M.J.; Wang, W.; Chan, C.Y.; Cheung, K.C.; Man, Y.B.; Wang, X.M.; Wong, M.H. Contamination and risk assessment (based on bioaccessibility via ingestion and inhalation) of metal(loid)s in outdoor and indoor particles from urban centers of Guangzhou, China. *Sci. Total Environ.* **2014**, *479*, 117–124. [CrossRef] [PubMed]
83. Cao, Z.G.; Chen, Q.Y.; Wang, X.Y.; Zhang, X.Y.; Wang, S.H.; Wang, M.M.; Zhao, L.C.; Yan, G.X.; Zhang, X.; Zhang, Z.Y.; et al. Contamination characteristics of trace metals in dust from different levels of roads of a heavily air-polluted city in north China. *Environ. Geochem. Health* **2018**, *40*, 2441–2452. [CrossRef]
84. Men, C.; Liu, R.M.; Xu, F.; Wang, Q.R.; Guo, L.J.; Shen, Z.Y. Pollution characteristics, risk assessment, and source apportionment of heavy metals in road dust in Beijing, China. *Sci. Total Environ.* **2018**, *612*, 138–147. [CrossRef]

85. Acosta, J.A.; Faz Cano, A.; Arocena, J.M.; Debela, F.; Martínez-Martínez, S. Distribution of metals in soil particle size fractions and its implication to risk assessment of playgrounds in Murcia City (Spain). *Geoderma* **2009**, *149*, 101–109. [CrossRef]
86. Jiang, Y.L.; Ma, J.H.; Ruan, X.L. Compound health risk assessment of cumulative heavy metal exposure: A case study of a village near a battery factory in Henan Province, China. *Environ. Sci. Process. Impacts* **2020**, *22*, 1408–1422. [CrossRef]
87. Lin, Z.; Ji, Y.Q.; Lin, Y.; Yang, Y.; Gao, Y.Z.; Wang, M.; Xiao, Y.; Zhao, J.Q.; Feng, Y.C.; Yang, W.; et al. PM10 and PM2.5 chemical source profiles of road dust over China: Composition, spatio-temporal distribution, and source apportionment. *Urban Clim.* **2023**, *51*, 101672. [CrossRef]
88. Wang, W.S.; Wang, N.; Gao, Y.J.; Zuo, R.T.; Ma, S.L.; Wang, J.J. Analysis of PM2.5 heavy pollution characteristics in spring and fall for 2019 in Zhengzhou. *Acta Sci. Circumstantiae* **2020**, *40*, 1594–1603, (In Chinese with English abstract).
89. Roy, M.; Ray, K.K.; Sundararajan, G. An analysis of the transition from metal erosion to oxide erosion. *Wear* **1998**, *217*, 312–320. [CrossRef]
90. Ameh, T.; Sayes, C. The potential exposure and hazards of copper nanoparticles: A review. *Environ. Toxicol. Pharmacol.* **2019**, *71*, 103220. [CrossRef]
91. Fergusson, J.E.; Kim, N.D. Trace elements in street and house dusts: Sources and speciation. *Sci. Total Environ.* **1991**, *100*, 125–150. [CrossRef]
92. Christoforidis, A.; Stamatis, N. Heavy metal contamination in street dust and roadside soil along the major national road in Kavala's region, Greece. *Geoderma* **2009**, *151*, 257–263. [CrossRef]
93. Zhang, J.; Deng, H.G.; Chen, Z.L.; Xu, S.Y. Heavy metal pollution in the urban street dust of Shanghai City. *Chin. J. Soil Sci.* **2007**, *38*, 727–731, (In Chinese with English abstract).
94. Lu, X.W.; Wang, L.J.; Li, L.Y.; Lei, K.; Huang, L.; Kang, D. Multivariate statistical analysis of heavy metals in street dust of Baoji, NW China. *J. Hazard. Mater.* **2010**, *173*, 744–749. [CrossRef]
95. Ahmed, F.T.; Khan, A.H.A.N.; Khan, R.; Saha, S.K.; Alam, M.F.; Dafader, N.C.; Sultana, S.; Elius, I.B.; Mamum, S.A. Characterization of As contaminated groundwater from central Bangladesh: Irrigation feasibility and preliminary health risks assessment. *Environ. Nanotechnol. Monit. Manag.* **2021**, *15*, 100433. [CrossRef]
96. Banerjee, A.D.K. Heavy metal levels and solid phase speciation in street dusts of Delhi, India. *Environ. Pollut.* **2003**, *123*, 95–105. [CrossRef]
97. Chen, X.; Lu, X.; Yang, G. Sources identification of heavy metals in urban topsoil from inside the Xi'an Second Ringroad, NW China using multivariate statistical methods. *Catena* **2012**, *98*, 73–78. [CrossRef]
98. Manoli, E.; Voutsa, D.; Samara, C. Chemical characterization and source identification/apportionment of fine and coarse air particles in Thessaloniki, Greece. *Atmos. Environ.* **2002**, *36*, 949–961. [CrossRef]
99. Harrison, R.M.; Tilling, R.; Callén Romero, M.S.; Harrad, S.; Jarvis, K. A study of trace metals and polycyclic aromatic hydrocarbons in the roadside environment. *Atmos. Environ.* **2003**, *37*, 2391–2402. [CrossRef]
100. Lu, X.W.; Wang, L.J.; Lei, K.; Huang, J.; Zhai, Y.X. Contamination assessment of copper, lead, zinc, manganese and nickel in street dust of Baoji, NW China. J. *Hazard. Mater.* **2009**, *161*, 1058–1062. [CrossRef]
101. Arslan, H. Heavy metals in street dust in Bursa, Turkey. *J. Trace Microprobe Tech.* **2001**, *19*, 439–445. [CrossRef]
102. Sun, Y.L.; Zhuang, G.S.; Zhang, W.J.; Wang, Y.; Zhuang, Y.H. Characteristics and sources of lead pollution after phasing out leaded gasoline in Beijing. *Atmos. Environ.* **2006**, *40*, 2973–2985. [CrossRef]
103. US EPA. *Soil Screening Guidance: Technical Background Document*; EPA/540/R-95/128; Office of Emergency and Remedial Response, U.S. Environmental Protection Agency: Washington, DC, USA, 1996.
104. Ministry of Ecology and Environment of the People's Republic of China. *Technical Guidelines for Risk Assessment of Contaminated for land for construction (HJ 25.3-2019)*; China Environmental Publishing Group: Beijing, China, 2019; pp. 49–50. (In Chinses)
105. Izquierdo, M.; Miguel, E.D.; Ortega, M.F.; Mingot, J. Bioaccessibility of metals and human health risk assessment in community urban gardens. *Chemosphere* **2015**, *135*, 312–318. [CrossRef] [PubMed]
106. Zhang, Z.Y.; Mamat, A.; Simayi, Z. Pollution assessment and health risks evaluation of (metalloid) heavy metals in urban street dust of 58 cities in China. *Environ. Sci. Pollut. Res.* **2019**, *26*, 126–140. [CrossRef]

Disclaimer/Publisher's Note: The statements, opinions and data contained in all publications are solely those of the individual author(s) and contributor(s) and not of MDPI and/or the editor(s). MDPI and/or the editor(s) disclaim responsibility for any injury to people or property resulting from any ideas, methods, instructions or products referred to in the content.